ACS Combinatorial Science

Letter

pubs.acs.org/acscombsci

High-Throughput Screening of Metal–Organic Frameworks for CO_2 Separation

Sangil Han, Yougui Huang, Taku Watanabe, Ying Dai, Krista S. Walton, Sankar Nair, David S. Sholl, and J. Carson Meredith*

School of Chemical & Biomolecular Engineering, Georgia Institute of Technology, 311 Ferst Drive, Atlanta, Georgia 30332-0100, United States

Supporting Information

ABSTRACT: A parallel high-throughput sorption methodology is described for screening CO_2 and N_2 adsorption and diffusion selectivity in metal organic frameworks, before and after exposure to water vapor and acid gases. We illustrate this approach by simultaneously investigating 8 candidate Metal–Organic Framework (MOF) materials, of which the best material was found to have a CO_2/N_2 membrane selectivity of 152 and a CO_2 permeability of 60 barrer for Co-NIC. This approach provides a significant increase in efficiency of obtaining the separation properties of MOFs. While we describe here the identification of novel materials for CO_2 capture, the methodology enables exploration of the performance and stability of novel porous materials for a wide range of applications.

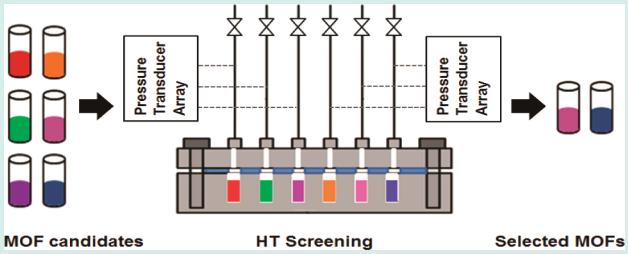

KEYWORDS: *CO_2 capture, adsorption, diffusion, sorption, acid gas, membrane*

The capture of CO_2 from fossil fuel combustion flue gas is the focus of significant research efforts. Existing CO_2 capture technologies such as amine absorption[1] are extremely energy intensive. Metal–organic frameworks (MOFs)[2] are potential size-selective, high-capacity materials for adsorptive and membrane-based capture of CO_2 and other gases.[3,4] MOFs exhibit nanoporous crystalline structure in which organic linker molecules self-assemble with metal centers to form crystals[5] with well-defined pore size, high surface area, and low framework density. MOFs have attracted attention as possible components of CO_2 capture technologies based on either adsorption or membranes.[6]

In principle, the enormous number of MOFs with various combinations of organic linker and metal cation creates an opportunity to tailor pore structure, size, and functionality for CO_2 capture from flue gas.[7] Significant problems, however, frustrate attempts to discover or design such materials. In addition to the large, under-explored design space, some MOFs are unstable in water vapor, and the principles for designing water-stable MOFs are not yet well-known.[8] The adsorption properties of a MOF are critical to its value for CO_2 capture. Measurements for determining adsorption isotherms are tedious and time-consuming. Almost all available data for gas adsorption in MOFs reports adsorption of dry single-component gases.[5] For considering practical CO_2 capture applications, the performance of MOFs that have been exposed to water vapor and acid gases like SO_2 and NO_2 is critical, and almost no data addressing this issue are available. There are few published reports of MOF stability after exposure to water[8,9] and none, to our knowledge, that examine stability as a function of exposure to acid gases.

To address the above challenges, we report here the efficient screening of MOF CO_2/N_2 adsorption and diffusion selectivity, as well as their sensitivity to water vapor and acid-gases, via the in-house design, construction, and use of a novel parallel high-throughput (HT) sorption screening system. Our HT approach differs from that reported recently by Wollmann et al.[10] which aims to rapidly assess the porosity of materials using a single adsorbate (*n*-butane). Instead, we collect adsorption information on the gases directly relevant to CO_2 capture (CO_2 and N_2) in the pressure regime relevant for flue gas applications. Similar to the approach of Wollman et al., a key element of our HT experiments is to collect adsorption data at only one relevant value of pressure, rather than measuring a complete adsorption isotherm. The HT-sorption instrument has an array of 36 chambers, each connected to a pressure sensor and a valve (Supporting Information). By monitoring pressure decay versus time, CO_2 and N_2 adsorption were measured at a single state point at 30 °C, which is in the middle of the range considered relevant to post-combustion CO_2 capture (20–40 °C).[11] In every case, the initial pressure in each chamber was 14.5 psi. The exact pressure at which equilibrium adsorption is measured depends on the uptake of gas into the sample, and is measured for every sample by each sensor at the end of the experiment (Supporting Information, Table S.1). The pressure

Received: February 14, 2012
Revised: March 13, 2012
Published: March 20, 2012

   dx.doi.org/10.1021/co3000192 | *ACS Comb. Sci.* 2012, 14, 263–267

range explored in these experiments, from 2.2 to 7.9 psi, is relevant to the partial pressure of CO_2 encountered in flue gas treatment, which is likely to be around a maximum of 3 psi. Because these low pressures fall in the Henry's regime, the pressure-corrected Henry's constants (described below) make comparison between the different chambers possible. As-synthesized MOF samples were activated at 120−200 °C under vacuum for 20 h. Small quantities (~100 mg) of each MOF sample were loaded into individual chambers of the HT screening system, and were degassed in vacuum for 20 h at 30 °C prior to every measurement (repeated in triplicate). Before using our HT apparatus to examine new MOFs, we first compared its results to previous adsorption data from several well-known materials. The ZIF-8 CO_2 adsorption capacity (0.22 mmol/g at 30 °C and 3.6 psi) observed with the HT screening system agreed very well with the previously reported capacity of 0.24 mmol/g at 25 °C and 3.6 psi.[12] The CO_2 uptake of ZIF-7 (0.24 mmol/g at 30 °C and 4.7 psi) observed with the HT system was consistent with the reported capacity (0.25 mmol/g)[13] at the same conditions. We also obtained good agreement between HT measurements and previous data for CO_2 and N_2 uptake in the pure-silica zeolite MFI and the polymer Matrimid (data not shown).

We selected eight MOF samples for testing (see Supporting Information): $\{[Zn_3(TTC)(OH)_2(H_2O)]\}_n \cdot 3H_2O$ (Zn-TTC), $\{[Zn(MeIm)_2]\}_n$ (ZIF-8), $[ZnCo(BTEC)(DMF)_2]_n$ (Zn/Co-BTEC), $\{[Zn(PhIM)_2 \cdot (H_2O)_3]\}_n$ (ZIF-7), $[Ni_2(hfpdpt)(bpy)_2(H_2O)_2](H_2O)_8$ (Ni-HF), $\{[Zn(ICA)_2]\}_n$ (ZIF-90), $\{[Co_2(NIC)_4(\mu\text{-}H_2O)] \cdot CH_3CH_2OH \cdot H_2O\}_n$ (Co-NIC), and $\{[Cu_2(PCN)_2(H_2O)_2]\}_n$ (Cu-PCN). These MOFs all have pore limiting diameters[14] (PLD, as obtained from their rigid crystal structures) smaller than the nominal kinetic diameter of N_2. These MOFs have a variety of organic linker functionalities, including CH_3, NO_2, C═O, and COOH. By choosing MOFs with relatively small pores (as identification of materials wherein diffusion of N_2 is strongly characterized by the PLD), we hypothesized the potentially hindered relative to CO_2. It is also reasonable to anticipate that CO_2 adsorption may be enhanced by polar functional groups.[15]

We first discuss the single component uptake of CO_2 and N_2 in the dried MOFs, prior to exposure to water vapor or acid gases. Figure 1 shows the observed dry CO_2 uptake for each material, to illustrate the shape of the data. Each sample reaches a different equilibrium pressure (Supporting Information, Table S.1) with different kinetics. To allow for meaningful comparisons, adsorbed amount is normalized by dividing by the equilibrium pressure, leading to units of mmol/g·psi. An average equilibrium uptake is calculated for each chamber after the pressure stopped changing, usually after 0.6 to 1 h. These uptakes are plotted in Figure 2a and 2b for CO_2 and N_2 adsorption, respectively. At the low pressures in our experiments, it is reasonable to assume that these quantities are Henry's constants for each MOF. This is convenient because in the Henry's regime, the adsorption selectivity, α, for a bulk gas mixture of any composition is simply the ratio of single component Henry's constants.[14] The resulting selectivities are listed in Table 1 and are plotted in Figure 2c, where the error bars indicate the standard deviations obtained from triplicate experiments. The three materials among the 8 tested with the highest CO_2/N_2 adsorption selectivity for dry gases are Co-NIC, Cu-PCN, and ZIF-7. No previous information on the adsorption selectivity of Co-NIC or Cu-PCN has been reported.

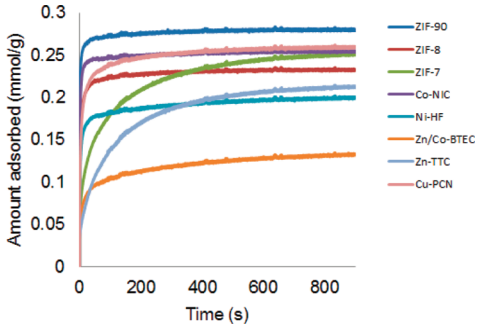

Figure 1. CO_2 uptake for 8 MOFs before water vapor exposure measured at 30 °C and initial pressure of 14.5 psi. Equilibrium pressures for each sample are different and are given in Supporting Information, Table S.1.

Brunauer−Emmett−Teller (BET) surface areas of the MOFs were measured at 77 K with liquid N_2 physisorption (Supporting Information, Table S.2). ZIF-8, ZIF-90, and Co-NIC showed BET surface areas of 1881, 654, and 297 m^2/g. The surface areas of Cu-PCN, Zn-TTC, Zn/Co-BTEC, Ni-HF, and ZIF-7 at 77 K were negligible. Table 1 shows, however, that all of these materials show N_2 uptake at 30 °C. The N_2 uptakes in Table 1 are much larger than can be accounted for by gas adsorption on the external surfaces of the crystals. These observations are consistent with strongly hindered diffusion of N_2 in the latter materials at low temperatures.

To probe the stability of each MOF, each material was exposed to air at 78% relative humidity (RH) and 26 °C for 3 days, near the 70% RH that has been used in previous work[11] for probing stability to humid air. The value of 78% was chosen for experimental convenience, since a saturated NaCl salt solution produces this value at 26 °C. The MOFs were then degassed by heating at 120 °C under vacuum for 1 day, and their equilibrium adsorption properties were measured. An additional adsorption experiment was performed after exposing each MOF to ~15 ppm SO_2 in air with 80% RH at 24 °C for 2 days and then ~10 ppm NO_2 in air with 80% RH at 24 °C for 2 days. Controlled levels of SO_2 and NO_2 were generated using the method of Hashimoto et al.[16] From the data in Table 1 and Figure 2, it is seen that most of the MOFs showed little change in adsorption uptake or selectivity after exposure to humid air. ZIF-90 was the only material that showed a decrease in adsorption selectivity, and this decrease was only 6%. The other materials showed increases in selectivity relative to adsorption prior to water vapor exposure, but these increases lie within the uncertainties of the measurements (see Figure 2c). The effects of acid gas exposure were more negative and dramatic. Zn/Co-BTEC showed the largest decrease in CO_2 uptake (−54%) and selectivity (−55%) after SO_2 and NO_2 exposure. ZIF-90, ZIF-8, ZIF-7, Co-NIC, and Ni-HF also showed reduced CO_2 and N_2 uptake and selectivities that decreased by 10−20% after SO_2 and NO_2 exposure. N_2 uptake of ZIF-90, ZIF-8, and ZIF-7 decreased by 7, 21, and 11% respectively. One material, Zn-TTC, showed adsorption properties that improved slightly after acid gas exposure. It is notable that the adsorption selectivity of ZIF-8 changed only slightly after exposure to acid gases, but the Henry's constants for both CO_2 and N_2 decreased significantly.

Each MOF was characterized by X-ray diffraction (XRD) before exposure to water vapor, after exposure to water vapor, and after exposure to acid gases (Supporting Information). Water vapor exposure did not lead to large changes in the XRD

dx.doi.org/10.1021/co3000192 | ACS Comb. Sci. 2012, 14, 263−267

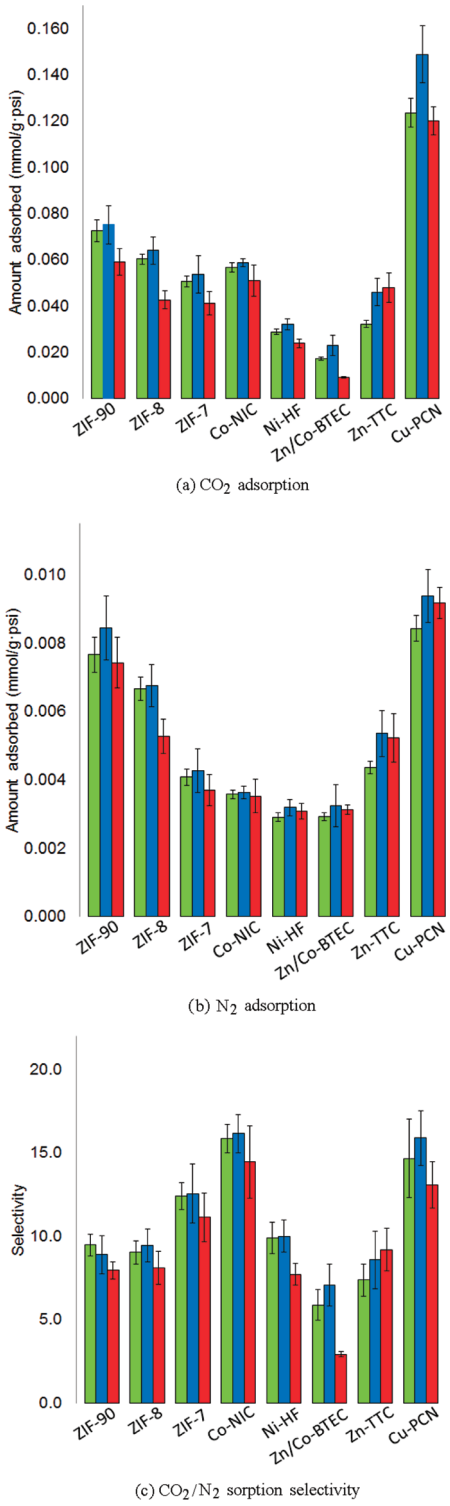

Figure 2. Pressure-corrected CO_2 (a) and N_2 (b) adsorption capacities (or Henry's constants) and CO_2/N_2 sorption selectivity, α, (c) before humid air (green), after humid air (blue), and after SO_2 and NO_2 exposure with humid air (red), measured at 30 °C and initial pressure of 14.5 psi. All data is normalized with respect to the equilibrium pressure for each sample and gas. Error bars represent standard deviation (n = 3).

patterns. The XRD patterns after SO_2 and NO_2 exposure did not show large changes for ZIF-8, Co-NIC, ZIF-7, and Cu-PCN, while ZIF-90 and Zn/Co-BTEC showed large decrease in the XRD peak intensities, indicating structural degradation. XRD patterns of Zn-TTC showed a crystalline structure, but the XRD pattern changed (Supporting Information, Figure S.10) after SO_2 and NO_2 exposure in humid air. This indicates that Zn-TTC transformed into a new and currently unidentified phase after acid gas exposure; Ni-HF showed degradation over time even without exposure to water vapor and the acid gas exposure while sealed in glassware at room temperature.

If a MOF (or any porous material) is to be used in an equilibrium-based adsorption separation, its performance is controlled solely by the adsorption isotherm. In membrane separations or kinetic-based adsorption separations, however, the relative diffusivities of the adsorbed species are also important.[5] Information on the effective diffusivity of adsorbing gases into samples in our HT apparatus can be determined from the kinetics of gas uptake. Diffusivity was estimated from a classical micropore diffusion model[17] (Supporting Information, Eq. S.1) assuming a spherical crystals with mass transfer resistance due to intracrystalline diffusion. The approximate solution[18] (Supporting Information, Eq. S.2) of this model relates fractional uptake to the diffusion time constant, D/r_c^2, where r_c is particle radius. Particle radii were estimated from SEM micrographs. Data with fractional uptake between 70 to 90% were used to calculate diffusion time constants.

The diffusion selectivity for each MOF sample was obtained from the ratio of the diffusion time constants for CO_2 and N_2. The results are summarized in Figure 3, and the estimated diffusivities are listed in Supporting Information, Table S.3. If CO_2 and N_2 diffused via Knudsen diffusion, as might be expected in large pore materials,[19] the CO_2/N_2 diffusion selectivity would be ~0.8. It is therefore noteworthy that all of the small pore MOFs we examined have diffusion selectivities larger than 1. Like the results for adsorption selectivity, most MOFs showed almost no change in diffusion selectivity after water vapor exposure. Only Ni-HF showed a significant decrease in diffusion selectivity after this exposure. Zn-TTC showed a large increase in diffusion selectivity after water vapor exposure, but this increase disappeared after exposure to acid gases. After SO_2 and NO_2 exposure, the diffusion selectivities of ZIF-8 and ZIF-7 decreased by 70% and 30%, respectively, primarily because of increased N_2 diffusivity. As is well-recognized,[20,21] determination of micropore diffusivity from uptake measurements is complicated by external mass transfer resistances and heat transfer resistances, which become increasingly important as particle size decreases. This requires the use of relatively large crystals for diffusivity measurements.[21,22] Our data for ZIF-90 come from crystals with r_c = 1.8 μm, and it is likely that these crystals were not large enough for our analysis to accurately describe intracrystalline diffusion. Results for the other 7 MOFs come from samples with r_c = 20–380 μm, wherein external resistances are likely to be minimal.

If a MOF is used in a membrane for CO_2/N_2 separation, the overall membrane selectivity can be estimated by the product of the adsorption and diffusion selectivities.[5] The resulting selectivity for each MOF is summarized in Supporting Information, Table S.4. The two materials with the most interesting results are Co-NIC and Cu-PCN, which have membrane selectivities of 152 and 83, because of their favorable sorption and diffusion selectivities. Importantly, we have shown that these materials are robust with respect to exposure to water vapor and/or acid gases. This is not true for all the materials examined. Exposing Zn/Co-BTEC to acid gases decreased its membrane selectivity from 32 to 13. ZIF-8 also showed a significant decrease in membrane selectivity from 15.3 to 5 after

dx.doi.org/10.1021/co3000192 | ACS Comb. Sci. 2012, 14, 263–267

Table 1. Henry's Constants (mmol/g psi, H_{CO2} and H_{N2}) and CO_2/N_2 Adsorption Selectivity (α) at 30 °C before and after Exposure to Humid Air and Acid Gases[a]

	before humid air			after humid air		after acid gases		selectivity change, %	
	H_{CO2}	H_{N2}	α	H_{CO2}	H_{N2}	H_{CO2}	H_{N2}	humid air	acid gases
ZIF-90	0.073	0.0077	9.5	0.075	0.0084	0.059	0.0074	−6	−13
ZIF-8	0.060	0.0067	9	0.064	0.0068	0.043	0.0053	6	−12
ZIF-7	0.051	0.0041	12.4	0.054	0.0043	0.041	0.0037	2	−11
Co-NIC	0.057	0.0036	15.9	0.059	0.0036	0.051	0.0035	2	−10
Ni-HF	0.029	0.0029	9.9	0.032	0.0032	0.024	0.0031	1	−20
Zn/Co-BTEC	0.017	0.0029	5.9	0.023	0.0032	0.009	0.0031	20	−55
Zn-TTC	0.032	0.0044	7.4	0.046	0.0054	0.048	0.0052	16	29
Cu-PCN	0.124	0.0084	14.7	0.149	0.0094	0.120	0.0092	8	−14

[a]Humid air with ~15 ppm SO_2 and then ~10 ppm NO_2.

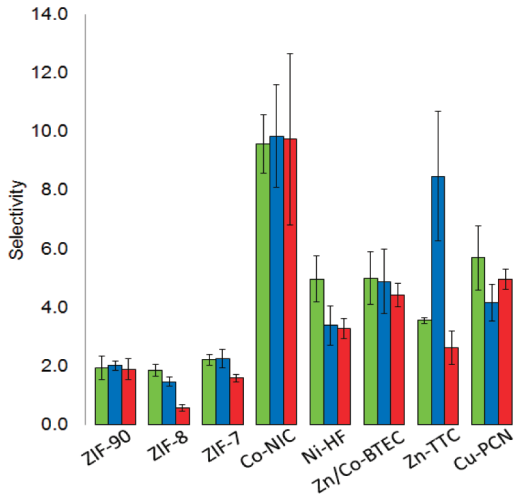

Figure 3. Diffusion selectivity measured at 30 °C. Green, blue, and red bars represent adsorption capacities before humid air, after humid air exposure, and after SO_2 and NO_2 exposure with humid air, respectively. Error bars represent standard deviation (n = 3).

SO_2 and NO_2 exposure. We emphasize that the membrane selectivities reported here are derived from measured adsorption and diffusion properties, not from direct observations with membranes.

In conclusion, we have demonstrated the feasibility of efficiently screening MOF materials in parallel on the basis of adsorption capacity, and adsorption and diffusion selectivities.[5] To our knowledge, this is the first high-throughput screening system which enables measurement of adsorption capacities and selectivities on MOFs, in addition to exposing the MOFs to water vapor and acid gases. The method leads to rapid selection of MOFs with high selectivity and stability to water vapor and acid gases. As a result, this paper reports data for acid gas stability previously unknown for these MOFs. The HT screening system can handle a variety of gas adsorbates and hence can be applied widely to screen adsorption and diffusion properties of other materials including inorganic compounds, polymers, and low-volatility liquids.

■ ASSOCIATED CONTENT

Supporting Information

MOF synthesis and structures, X-ray diffraction data, and other experimental details. This material is available free of charge via the Internet at http://pubs.acs.org.

■ AUTHOR INFORMATION

Corresponding Author

*Phone: +1) 404-385-2151. Fax: +1) 404-894-2866. E-mail: carson.meredith@chbe.gatech.edu.

Funding

We gratefully acknowledge support from the DOE ARPA-E IMPACCT program under Grant DE-AR0000074.

Notes

The authors declare no competing financial interest.

■ REFERENCES

(1) Cui, Z.; Aroonwilas, A.; Veawab, A. Simultaneous Capture of Mercury and CO_2 in Amine-Based CO_2 Absorption Process. *Ind. Eng. Chem. Res.* **2010**, *49*, 12576.
(2) Rowsell, J. L. C.; Yaghi, O. M. Metal−Organic Frameworks: a New Class of Porous Materials. *Micro. Meso. Mater.* **2004**, *73*, 3.
(3) Morris, R. E.; Wheatley, P. S. Gas Storage in Nanoporous Materials. *Angew. Chem., Int. Ed.* **2008**, *47*, 4966.
(4) Horcajada, P.; Serre, C.; Maurin, G.; Ramsahye, N. A.; Balas, F.; Vallet-Regì, M.; Sebban, M.; Taulelle, F.; Férey, G. Flexible Porous Metal-Organic Frameworks for a Controlled Drug Delivery. *J. Am. Chem. Soc.* **2008**, *130*, 6774.
(5) Keskin, S.; van Heest, T. M.; Sholl, D. S. Can Metal−Organic Framework Materials Play a Useful Role in Large-Scale Carbon Dioxide Separations? *ChemSusChem* **2010**, *3*, 879.
(6) Banerjee, R.; Furukawa, H.; Britt, D.; Knobler, C.; O'Keeffe, M.; Yaghi, O. M. Control of Pore Size and Functionality In Isoreticular Zeolitic Imidazolate Frameworks and Their Carbon Dioxide Selective Capture Properties. *J. Am. Chem. Soc.* **2009**, *131*, 3875.
(7) Zhao, D.; Timmons, D. J.; Yuan, D.; Zhou, H. Tuning the Topology and Functionality of Metal−Organic Frameworks by Ligand Design. *Acc. Chem. Res.* **2011**, *44*, 123.
(8) Low, J. J.; Benin, A. I.; Jakubczak, P.; Abrahamian, J. F.; Faheem, S. A.; Willis, R. R. Virtual High Throughput Screening Confirmed Experimentally: Porous Coordination Polymer Hydration. *J. Am. Chem. Soc.* **2009**, *131*, 15834.
(9) Liang, Z.; Marshall, M.; Chaffee, A. L. CO_2 Adsorption-Based Separation by Metal Organic Framework (Cu-BTC) versus Zeolite (13X). *Energy Fuels* **2009**, *23*, 2785.
(10) Wollmann, P.; Leistner, M.; Stoeck, U.; Grünker, R.; Gedrich, K.; Klein, N.; Throl, O.; Grählert, W.; Senkovska, I.; Dreisbach, F.; Kaskel, S. High-throughput Screening: Speeding Up Porous Materials Discovery. *Chem. Commun.* **2011**, *47*, 5151.
(11) Sumida, K.; Rogow, D. L.; Mason, J. A.; McDonald, T. M.; Bloch, E. D.; Herm, Z. R.; Bae, T.; Long, J. R. Carbon Dioxide Capture in Metal-Organic Frameworks. *Chem. Rev.* **2012**, *122*, 724.
(12) Yazaydın, A. O.; Snurr, R. Q.; Park, T.; Koh, K.; Liu, J.; LeVan, M. D.; Benin, A. I.; Jakubczak, P.; Lanuza, M.; Galloway, D. B.; Low, J. J.; Willis, R. R. Screening of Metal-Organic Frameworks for Carbon

Dioxide Capture from Flue Gas using a Combined Experimental and Modeling Approach. *J. Am. Chem. Soc.* **2009**, *131*, 18198.
(13) Aguado, S.; Bergeret, G.; Titus, M. P.; Moizan, V.; Nieto-Draghi, C.; Batsb, N.; Farrusseng, D. Guest-Induced Gate-Opening of a Zeolite Imidazolate Framework. *New J. Chem.* **2011**, *35*, 546.
(14) Haldoupis, E.; Nair, S.; Sholl, D. S. Efficient Calculation of Diffusion Limitations in Metal Organic Framework Materials: A Tool for Identifying Materials for Kinetic Separations. *J. Am. Chem. Soc.* **2010**, *132*, 7528.
(15) Bae, Y.; Farha, O. K.; Hupp, J. T.; Snurr, R. Q. Enhancement of CO_2/N_2 Selectivity in a Metal-Organic Framework by Cavity Modification. *J. Mater. Chem.* **2009**, *19*, 2131.
(16) Hashimoto, Y.; Tanaka, S. A New Method of Generation of Gases at Parts Per Million Levels for Preparation of Standard Gases. *Environ. Sci. Technol.* **1980**, *14*, 413.
(17) Bao, Z.; Yu, L.; Ren, Q.; Lu, X.; Deng, S. Adsorption of CO_2 and CH_4 on a Magnesium-Based Metal Organic Framework. *J. Colloid Interface Sci.* **2011**, *353*, 549.
(18) Saha, D.; Bao, Z.; Jia, F.; Deng, S. Adsorption of CO_2, CH_4, N_2O, and N_2 on MOF-5, MOF-177, and Zeolite 5A. *Environ. Sci. Technol.* **2010**, *44*, 1820.
(19) Skoulidas, A. I.; Sholl, D. S. Self-Diffusion and Transport Diffusion of Light Gases in Metal-Organic Framework Materials Assessed using Molecular Dynamics Simulations. *J. Phys. Chem. B* **2005**, *109*, 15760.
(20) Ruthven, D. M. *Principles of Adsorption and Adsorption Processes*; Wiley-Interscience: New York, 1984.
(21) Conner, W. C.; Fraissard, J. *Fluid Transport in Nanoporous Materials*; Springer: La Colle sur Loup, France, 2006.
(22) Sun, M. S.; Talu, O. S.; Shah, D. B. Diffusion Measurements through Embedded Zeolite Crystals. *AIChE J.* **1996**, *42*, 3001.